

# Radiation characterization summary of the NETL beam port 1/5 free-field environment at the 128-inch core centerline adjacent location

*Danielle Redhouse*<sup>1,\*</sup>, *William Charlton*<sup>2</sup>, *Edward Parma*<sup>3</sup>, *Curtis Peters*<sup>1</sup>, *Mark Andrews*<sup>2</sup>, *Jesse Roebuck*<sup>1</sup>, and *Ryan Mulcahy*<sup>1</sup>

<sup>1</sup>Sandia National Laboratories, Albuquerque, NM, USA

<sup>2</sup>University of Texas at Austin, Austin, TX, USA

<sup>3</sup>Sandia National Laboratories (Retired), Albuquerque, NM, USA

**Abstract.** The characterization of the neutron, prompt gamma-ray, and delayed gamma-ray radiation fields in the University of Texas at Austin Nuclear Engineering Teaching Laboratory (NETL) TRIGA reactor for the beam port (BP) 1/5 free-field environment at the 128-inch location adjacent to the core centerline has been accomplished. NETL is being explored as an auxiliary neutron test facility for the Sandia National Laboratories radiation effects sciences research and development campaigns. The NETL reactor is a TRIGA Mark-II pulse and steady-state, above-ground pool-type reactor. NETL is intended as a university research reactor typically used to perform irradiation experiments for students and customers, radioisotope production, as well as a training reactor. Initial criticality of the NETL TRIGA reactor was achieved on March 12, 1992, making it one of the newest test reactor facilities in the US. The neutron energy spectra, uncertainties, and covariance matrices are presented as well as a neutron fluence map of the experiment area of the cavity. For an unmoderated condition, the neutron fluence at the center of BP 1/5, at the adjacent core axial centerline, is about  $8.2 \times 10^{12}$  n/cm<sup>2</sup> per MJ of reactor energy. About 67% of the neutron fluence is below 1 keV and 22% above 100 keV. The 1-MeV Damage-Equivalent Silicon (DES) fluence is roughly  $1.6 \times 10^{12}$  n/cm<sup>2</sup> per MJ of reactor energy.

---

\* Corresponding author: [dredho@sandia.gov](mailto:dredho@sandia.gov)

## 1 Introduction

Characterization of the neutron and gamma-ray environments in the University of Texas at Austin's (UT-Austin) Nuclear Engineering Teaching Laboratory (NETL) is important to maintain a high degree of fidelity in experimentation and testing [1]. The NETL reactor is a TRIGA Mark-II pulse and steady-state, above ground pool-type reactor. NETL is located at the J.J. Pickle Research Center at UT-Austin in Austin, Texas. UT-Austin previously operated a TRIGA reactor on the UT-Austin main campus from 1963 to 1988. The fuel from the previous TRIGA reactor was moved to the current reactor location, and construction on the current reactor began in 1986. Initial criticality of the NETL TRIGA reactor was achieved on March 12, 1992.

NETL is a university research reactor typically used to perform irradiation experiments for students and customers, radioisotope production, as well as a training reactor. Historically, NETL has been used for a wide variety of experiment campaigns including radiation damage in materials testing, neutron radiography, neutron activation analysis, prompt gamma-ray activation analysis, and radioisotope production of xenon (Xe). NETL is being explored as an auxiliary neutron test facility for the Sandia National Laboratories (SNL) Radiation Effects Sciences Campaigns as well as a prototyping facility.

The neutron energy spectra and uncertainties are presented at the axial center of beam port 1/5 (BP 1/5) at the axial fuel centerline adjacent to the reactor core, the peak neutron fluence location. In addition, radial and axial neutron fluence profiles are given within the available experiment area inside of the beam port. Recommended constants are given that facilitate the conversion of various dosimetry readings into radiation metrics desired by experimenters.

## 2 Environment Description

The fuel elements for NETL are the standard uranium zirconium hydride (UZrH) TRIGA fuel [16]. NETL is fueled by a hexagonal array of UZrH fuel elements. There are 116 possible fuel locations in the reactor with the core currently operating with 113 fuel elements. The fuel uses uranium enriched to 19.5 weight percent U-235. The UZrH contains a fine metallic dispersion of uranium in a ZrH matrix, with 8.5% of the mass of the fuel material as uranium. The H:Zr ratio is nominally 1.6. The NETL fuel elements are stainless steel clad, 37.5 mm (1.47 inches) in diameter and 721.3 mm (28.4 inches) in length. The fuel meat is 36.4 mm (1.43 inches) in diameter and 381.0 mm (15.0 inches) long. NETL is controlled by two fuel-followed shim safety rods, one fuel-followed regulating rod, and one void-followed transient rod. The control rods are positioned in four fuel locations in the normal core configuration.

NETL's main irradiation facilities include five dry beam port irradiation locations, a rotary specimen rack, a pneumatic rabbit system, two in-core dry irradiation locations for use with the pneumatic rabbit system, two in-core three-element cut-out locations, two in-core seven-element cut-out locations, and a wet central thimble element. The NETL fission rate is driven by thermal neutrons and therefore most of the irradiation locations feature a strong thermal neutron flux. NETL does maintain four irradiation modifying capabilities that utilize absorbers such as cadmium or boron to remove thermal and epithermal neutrons. NETL has capabilities for pulsing operations and steady-state operations for reactor power levels between 0.1 kW and 1100 kW.

Figure 1 shows the NETL reactor looking into the pool (during a low-power steady-state power operation). The NETL core is shown in the center of the figure. The five beam ports are shown with the BP 1/5 through port shown extending from the top center to the bottom left. Each beam port is a dry cavity with a diameter of about 152.4 mm (6 inches). The beam port locations are tubing that traverse the reactor pool, with the radius of the tubes being smallest near the reactor core. Each beam port space allows installation of experiment assemblies at the center of the port either normal or adjacent to the core, where neutron fluence levels are highest. BP 1/5 starts as a stainless-steel cavity and transitions to aluminum to allow for minimal neutron activation and interaction. Within this beam port, experiments can be adjusted axially through the use of pedestals or sleds.

In the steady-state mode, the operating power level is limited to  $\sim 1.1$  MW. In the pulse mode, a maximum pulse size of  $\sim 23$  MJ with a full-width half-maximum (FWHM) of 12 ms can be attained. In the square-wave pulse mode, the reactor is ramped to a desired power level ( $< 1.1$  MW), power is maintained via automated control system for a prescribed time period, and then power is rapidly decreased to shutdown. This procedure results in a square pulse shape and can be tailored to the desired requirements for higher total reactor energy depositions.

The coupling factor is defined as the amount of fission energy that can be produced in a fissile experiment per gram of fissile fuel and per MJ of reactor power. The coupling factor for the unmoderated BP 1/5 is  $\sim 7.9$  J/g-MJ. These coupling factors allow for fueled experiments to be designed for a wide variety of test conditions for steady-state and pulse operations.

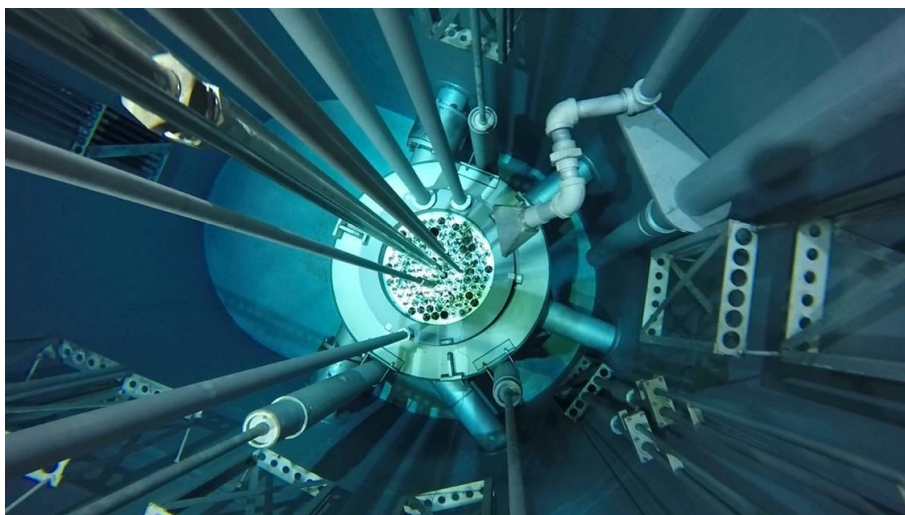


**Fig. 1.** Top View NETL reactor and core pool.

### 3 Neutronics Model

Characterizations include both modeling and experimental efforts. Accurate neutronic models of NETL and the beam port environments can be used by experimenters, for planning and designing experiments, and in assessing experimental results. Experimental observations, including passive and active dosimetry, are important in order to determine

the accuracy of the model, the energy dependent neutron fluence, the conversion constants for radiation metrics, and time-dependent responses for different pulse sizes.

The neutronics model for NETL used in the BP 1/5 free-field characterization was developed for the Monte Carlo N-Particle Transport Code X (MCNPX) Version [4]. The NETL MCNP model was assembled by P. Michael Whaley (NETL) and later modified by William Charlton (NETL) for modern MCNP. Further alterations to NETL MCNP model were done by Danielle Redhouse and Curtis Peters (SNL) in 2020. A 640-group and 89-group neutron energy spectrum was calculated using MCNP 6.2 and the ENDF/B-VIII.0 cross sections for the NETL model with a scoring sphere at the radial centerline of the beam port at the axial centerline of the core.

The MCNP model of the NETL reactor and its five beam ports is shown in Figure 2. The model includes all the fuel elements as well as the control and safety rods that make up the core. The control and safety rods can be adjusted in the vertical direction in the model to whatever position is desired. Typically, the model is run with the shim safety and transient rods banked to the same height for the approximately delayed critical (dc) position. The calculated dc position can be found for the model by iterating on the control rod position until  $k_{\text{eff}}$  is equal to one. The model is typically run using room-temperature (300 K) cross sections,  $S(\alpha, \beta)$  values, and water density.

Neutron energy spectra and fluence per fission were calculated using a 6-cm diameter tally sphere, positioned at the radial center of the cavity at the axial centerline of the beam port, which is core adjacent. Calculations were performed using the MCNP k-code mode [4]. In order to have reasonable statistics in all of the energy groups, the model was run on a parallel machine for 20 billion source neutrons. The neutron fluence results were converted from fluence per fission to fluence per MJ of reactor power using 192.4 MeV per fission. This value represents the fission fragment, neutron, prompt gamma-ray, capture gamma-ray and delayed gamma-ray energy deposition in the reactor core and surrounding water, per fission event [8].

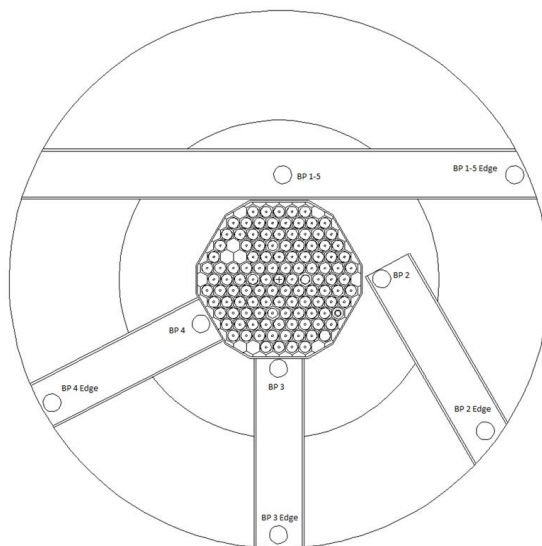


**Fig. 2.** MCNP Model of the NETL Core and beam ports in the reactor pool with tally spheres.

## 4 Experiment and Dosimetry

The neutron environment includes both prompt and delayed neutrons from NETL core. The neutron energy spectrum is first calculated using MCNP and then a least-squares spectrum adjustment is performed using passive neutron activation dosimetry measurements to produce a “characterized” neutron spectrum [13]. For this work a total of 22 different dosimetry foil types, resulting in 42 different transmutation reactions, were irradiated at the center of the BP 1/5, called the NETL-FF-BP1/5-128-cca location. The LSL-M3 code and the IRDFF-II dosimetry cross sections were used in the unfolding analysis to determine the characterized neutron energy spectrum [5][14].

A considerable uncertainty in MCNP results exists due to model representation uncertainty (geometry, density, and composition) and uncertainty in the transport cross sections. An improved spectrum is obtained by combining this initial spectrum with measured integral values that correspond to the reaction rates from high-fidelity passive dosimetry reactions. The selected set of passive dosimetry foils and activation reactions has been studied and evaluated over many years, and summaries of these works can be found in ASTM E720 and works reference in this paper [7][9][10]. Currently, no complete or perfect set of activation reactions exists that allows the neutron fluence energy spectrum to be calculated by dosimetry alone. However, there are enough reactions to cover the relevant energy range with high-fidelity dosimetry cross sections to allow for adjusted neutron fluence results to be generated with a quantified accuracy [2][11].

For this work a total of 22 different foil types, resulting in 42 different reactions, were irradiated in the previously described BP 1/5 environment. The passive dosimetry foils and the associated neutron activities, at end of irradiation, used to perform the neutron fluence characterization for the free-field environment are shown in Table 1.

**Table 1.** Neutron Activation Dosimetry Used for NETL-FF-BP1/5-128-cca [2].

Activation Reaction	Half-Life	Specific Activity (Bq/atom-isotope)	Counting Uncertainty (%)
$^{58}\text{Ni}(n,p)^{58}\text{Co}$ - Reference	70.86 d	3.8026E-19	2.11
$^{24}\text{Mg}(n,p)^{24}\text{Na}$	14.957 h *	6.0257E-19	0.05
$^{27}\text{Al}(n,\alpha)^{24}\text{Na}$	14.957 h *	2.4885E-19	3.75
$^{24}\text{Al}(n,p)^{27}\text{Mg}$	9.462 m *	1.1924E-16	2.56
$^{32}\text{S}(n,p)^{32}\text{P}$ Cf-equ	14.284 d	1.865E+12 n/cm <sup>2</sup>	1.05
$^{46}\text{Ti}(n,p)^{46}\text{Sc}$	84.79 d	2.9902E-20	3.75
$^{47}\text{Ti}(n,p)^{47}\text{Sc}$	3.345 d	1.2844E-18	2.08
$^{48}\text{Ti}(n,p)^{48}\text{Sc}$	43.67 h	3.3129E-20	1.31
$^{54}\text{Fe}(n,p)^{54}\text{Mn}$	312.3 d	5.2798E-20	3.71
$^{56}\text{Fe}(n,p)^{56}\text{Mn}$	2.578 h *	2.2592E-18	3.48
$^{58}\text{Ni}(n,2n)^{57}\text{Ni}$	35.65 h	2.3033E-21	15.76
$^{60}\text{Ni}(n,p)^{60}\text{Co}$	1925.5 d	1.4355E-21	7.03
$^{90}\text{Zr}(n,2n)^{89}\text{Zr}$	78.41 h	5.4908E-20	26.72
$^{115}\text{In}(n,n')^{115\text{m}}\text{In}$	4.486 h *	9.0043E-18	2.15
$^{115}\text{In}(n,2n)^{114\text{m}}\text{In}$	49.51 d	1.6917E-16	1.74

$^{23}\text{Na}(n,\gamma)^{24}\text{Na}$	14.9654 h *	4.8116E-16	3.42
$^{45}\text{Sc}(n,\gamma)^{46}\text{Sc}$	84.79 d	2.5889E-16	2.11
$^{55}\text{Mn}(n,\gamma)^{56}\text{Mn}$	2.5785 h *	9.1375E-14	2.26
$^{58}\text{Fe}(n,\gamma)^{59}\text{Fe}$	44.496 d	2.1729E-17	1.60
$^{59}\text{Co}(n,\gamma)^{60}\text{Co}$	1925.5 d	1.5123E-17	2.44
$^{63}\text{Cu}(n,\gamma)^{64}\text{Cu}$	12.701 h *	6.7252E-15	2.50
$^{93}\text{Nb}(n,\gamma)^{94\text{m}}\text{Nb}$	6.263 m *	2.4082E-09	1.27
$^{96}\text{Zr}(n,\gamma)^{97}\text{Zr}$	16.744 h*	3.4434E-16	2.03
$^{98}\text{Mo}(n,\gamma)^{99}\text{Mo}$	65.94 h	1.5474E-16	2.37
$^{109}\text{Ag}(n,\gamma)^{110\text{m}}\text{Ag}$	249.76 d	1.6455E-17	1.91
$^{115}\text{In}(n,\gamma)^{116\text{m}}\text{In}$	54.41 m *	2.2301E-12	1.81
$^{186}\text{W}(n,\gamma)^{187}\text{W}$	23.9 h *	3.9707E-14	1.80
$^{197}\text{Au}(n,\gamma)^{198}\text{Au}$	2.6943 d	3.6426E-14	2.14
$^{23}\text{Na}(n,\gamma)^{24}\text{Na} - \text{Cd}$	14.9654 h *	2.1049E-17	3.43
$^{45}\text{Sc}(n,\gamma)^{46}\text{Sc} - \text{Cd}$	84.79 d	5.9782E-18	2.28
$^{55}\text{Mn}(n,\gamma)^{56}\text{Mn} - \text{Cd}$	2.5785 h *	3.6905E-15	1.81
$^{58}\text{Fe}(n,\gamma)^{59}\text{Fe} - \text{Cd}$	44.496 d	1.0682E-18	2.36
$^{59}\text{Co}(n,\gamma)^{60}\text{Co} - \text{Cd}$	1925.5 d	1.0340E-18	2.53
$^{63}\text{Cu}(n,\gamma)^{64}\text{Cu} - \text{Cd}$	12.701 h *	2.5189E-16	2.07
$^{98}\text{Mo}(n,\gamma)^{99}\text{Mo} - \text{Cd}$	65.94 h	9.0848E-17	2.55
$^{109}\text{Ag}(n,\gamma)^{110\text{m}}\text{Ag} - \text{Cd}$	249.76 d	3.1107E-18	1.91
$^{197}\text{Au}(n,\gamma)^{198}\text{Au} - \text{Cd}$	2.6943 d	1.3851E-14	1.46
$^{235}\text{U}(n,f)\text{FP} - \text{Bare}$	$^{140}\text{Ba} - 12.752 \text{ d}$	9.7601E-11 #fiss	1.64
$^{238}\text{U}(n,f)\text{FP} - \text{Bare}$	$^{140}\text{Ba} - 12.752 \text{ d}$	9.9184E-12 #fiss	1.22
$^{237}\text{Np}(n,f)\text{FP} - \text{Bare}$	$^{140}\text{Ba} - 12.752 \text{ d}$	5.9570E-11 #fiss	1.67
$^{239}\text{Pu}(n,f)\text{FP} - \text{Bare}$	$^{140}\text{Ba} - 12.752 \text{ d}$	1.0853E-10 #fiss	1.64

Typically, neutron activation resulting in the emission of protons (n,p), neutrons (n,2n), (n,n'), or alpha particle (n, $\alpha$ ) represent high neutron-energy reactions of 1 MeV or greater. Neutron activation resulting in prompt gamma-ray emission from radiative capture (n, $\gamma$ ) or fission reactions inform the shape of the thermal and epithermal region of the neutron spectrum. Covering foils with cadmium can allow for resonances above the associated cut-off energies to become more prominent, allowing for additional information to be included in the analysis.

The foils were irradiated in three different maximum pulse (23 MJ) operations. The four fission foils (U-235, U-238, Pu-239, and Np-237) were irradiated together in a free-field configuration in one pulse operation. Three foils (In, Mo, Nb) were also irradiated but were not used in the analysis due to significant inconsistencies in the unfolding results. It is unknown at this time if there are problems in the measurement technique for these reactions, foil pre-exposure issues, or if there are issues with the dosimetry cross sections. Figure 3 shows a picture of some of the dosimetry foils used, from left to right, top to bottom: Nb, Mn, Al, Co, Sc, NaCl, Cu, Ni-28, Au, Fe, Ti, Zr, Mg, W, Zn, Co, Ag, and In. For reference, the nickel (Ni) (28, 29) foils are typically 1.27 cm (0.5 inches) in diameter. The irradiations were all performed at the peak axial neutron fluence location within the

beam port. Multiple foils were irradiated on a specially designed aluminum stand, which held the foils at the 128-inch position in the beam port. In order to minimize any self-shielding effects, the foils were never stacked together. Instead, the foils were arranged on the surface of an aluminum plate held in place with tape. For each irradiation, at least one nickel foil was irradiated and used to normalize all the irradiations.

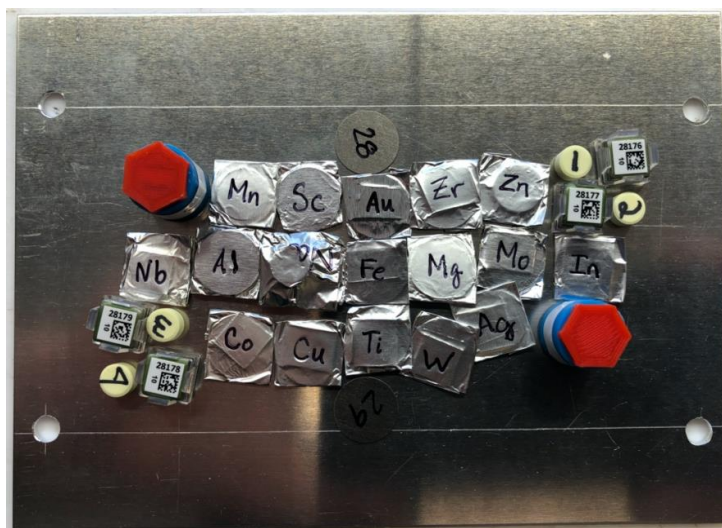


**Fig. 3.** Typical Dosimetry Foils – Characterization Test Setup.

The free-field environment was used to perform all the foil irradiations identified in Table 1. High variation in the flux was found radially and axially within the BP 1/5 position. However, a test region where the neutron fluence varied by only  $\pm 5\%$  was identified. Careful testing considerations should be made when testing in beam port 1/5. Additional uncertainty in the analysis was included to account for possible variation due to geometry effects.

The free-field environment requires adequate coverage of the thermal, epithermal, and high-energy neutron reactions in order to perform a successful adjustment to the neutron fluence energy spectrum. Cd covers are used to discriminate energy regions in some reactions. Table 1 shows each activation reaction used in the analysis, as well as the half-life for the transmuted isotope, the measured activity decay corrected to the end of the irradiation, and the counting uncertainty. The reactions are grouped in order of reaction type. The first group represents the high-energy (n,p), (n,2n), (n,n'), and (n,  $\alpha$ ) reactions. The second group represents the low-energy radiative capture reactions for bare foils. The third group represents the radiative capture reactions with each individual foil placed in a cadmium cover. The fourth group represents the fission foils. Reactions identified with a dark-gray colored box in Table 1 represent reactions that were not used in the final spectrum adjustment due to inconsistencies in the results.

## 5 Spectrum Characterization

The LSL-M3 code was run using the *a priori* 640-energy group trial spectrum from MCNP converted to the NuGET 89-energy group structure, and the dosimetry data

presented in Table 1. Also required in the analysis was an initial uncertainty estimate in the neutron spectrum as a function of energy, an initial energy-dependent correlation matrix, the energy dependent self-shielding factors, and the dosimetry cross section library that also included uncertainties and covariance matrices. In addition to the counting uncertainty, an additional 2% uncertainty was included for the foils to address uncertainty contributions due to positioning and possible geometrical effects in the central region of the beam port. The output is the 89-energy group NuGET format described earlier.

The resulting value for the chi-squared per degrees of freedom is 1.013, which represents an acceptable value. Figure 4 and Figure 5 show the same representation of the neutron energy spectra from the MCNP neutronic models with the additional 89-energy group adjusted spectrum result from the LSL analysis (blue curve).

For an unmoderated condition, the neutron fluence at the center of BP. 1/5, at the adjacent core axial centerline, is  $\sim 8.2E+12$  n/cm<sup>2</sup> per MJ of reactor energy. About 67% of the neutron fluence is below 1 keV and 22% above 100 keV. The 1-MeV Damage-Equivalent Silicon (DES) fluence is  $\sim 1.6E+12$  n/cm<sup>2</sup> per MJ of reactor energy. The prompt gamma-ray dose at the same position is  $\sim 2.5E+03$  rad(Si) per MJ. The delayed gamma-ray dose is  $\sim 9.6E+02$  rad(Si) per MJ[8].

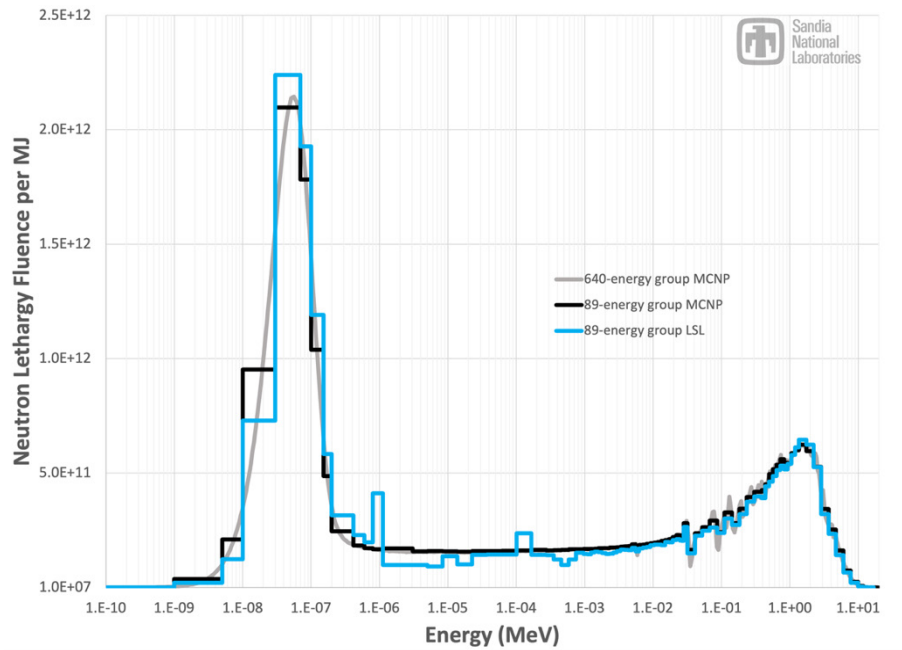


**Fig. 4.** LSL Adjusted 89-Group Neutron Lethargy Fluence Energy Spectrum Compared to the MCNP Calculated Results (linear-log).



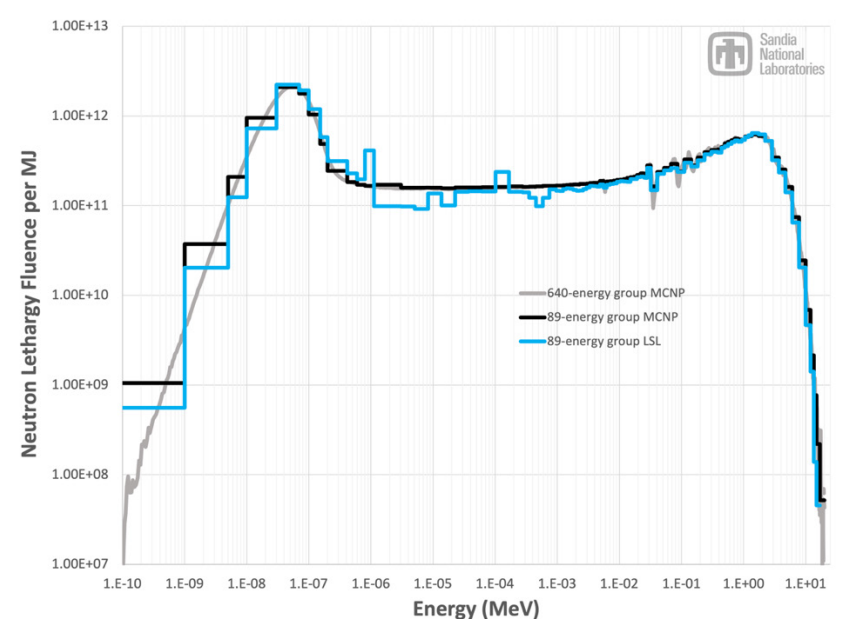


**Fig. 5.** LSL Adjusted 89-Group Neutron Lethargy Fluence Energy Spectrum Compared to the MCNP Calculated Results (log-log).

The peak differential number fraction occurs in energy group 5 at 0.03 eV. The differential fluence at 1 MeV (Group 74) is almost three orders of magnitude lower than the peak. The differential energy fluence for the same comparison is about the same order of magnitude as for the 1 MeV value. The results for several integral metrics and conversion factors are shown in Table 2. The total neutron fluence is normalized to 1.00, and the other values for fluence are in reference to this value. These values were calculated as part of the LSL analysis. Conversion values to translate to  $n/cm^2$  are given for fissions in the reactor, MJ of reactor energy, and  $^{58}Ni(n,p)^{58}Co$  activity at the characterized location in the cavity. In order to maintain consistency, the experimenter should always use a reference fast neutron reaction or reactions, e.g.,  $^{58}Ni(n,p)^{58}Co$  and  $^{32}S(n,p)^{32}P$ , as a normalizing metric between operations. Typically, Ni, S, and TLD sensors are included in an experiment package in order to normalize the results of the experiment.

Table 2 also shows representative integral metrics that may be useful to experimenters. These values were calculated using the LSL adjusted 89-energy group neutron spectrum and the SNL NuGET code with various response functions [6]. Passive dosimetry was used to determine the axial and radial neutron profiles. This irradiation of dosimetry was performed in the BP 1/5 through port free-field environment at the radial centerline of the beam port at the axial centerline of the core that is core centerline adjacent, roughly 128-inches into either entrance of the beam port. Figure 6 shows a model of the dosimetry fixture.

**Table 2.** Integral Neutron Spectrum Metrics, Total Ionizing Dose Metrics, and Associated Uncertainties.

Metric	Integral Response	Standard Deviation (%)
Total Neutron Fluence Average Neutron Energy = 0.302 MeV	1.00	---
Fluence > 3 MeV	0.024	3.0
Fluence > 1 MeV	0.101	3.4
Fluence > 100 keV	0.218	3.0
Fluence > 10 keV	0.282	2.8
Fluence < 1 eV	0.534	15.8
Fluence 1-MeV(Si) Eqv. E722-19 (Ref. 1-MeV value = 95 MeV-mb)	18.5 MeV-mb 0.195	2.9
Total Fluence Conversion ([n/cm <sup>2</sup> ]/fission)	2.527E-04	0.3
Total Fluence Conversion ([n/cm <sup>2</sup> ]/MJ)	1.094E+13	2.2
Metric	Integral Reponse	
Total Neutron Silicon Dose (rad <sub>n</sub> [Si]/MJ)	1.626E+02	
Ionizing Neutron Silicon Dose (rad <sub>n</sub> [Si]/MJ)	9.420E+01	
Percent Neutron Si Dose Ionizing (%)	57.9	
Ionizing Prompt Gamma-Ray Silicon Dose (rad <sub>γ</sub> [Si]/MJ)	2.527E+03	
Ionizing Delayed Gamma-Ray Silicon Dose (rad <sub>dγ</sub> [Si]/MJ)	9.641E+02	
Total Ionizing Silicon Dose (rad[Si]/MJ)	3.585E+03	

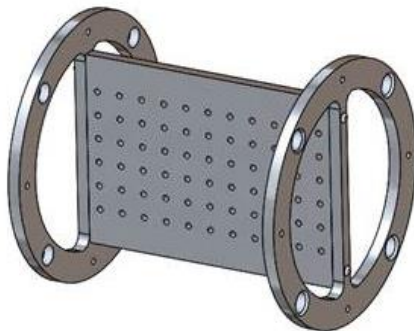


**Fig. 6.** Mapping Fixture used in Beam Port 1/5.

Figure 7 shows the normalized results for the sulfur axial and radial neutron fast fluence profile on the test fixture that is commonly used in BP 1/5. In this image, a value of 1 indicates that the neutron metrics noted above are unchanged. The results show that over a majority of the test fixture, the fluence magnitude varies by only  $\pm 5\%$ , with slightly higher

fluence rates favoring the top of the test fixture. For reference, the axial fuel centerline is ~6.985 cm (2.75 inches) from the top of the 6-inch BP 1/5 fixture. The NETL fuel is 52.25 cm (20.57 inches) in length.



Fig. 7. Sulfur Map for the NETL-FF-BP1/5-128-cca test fixture.

## 6 Conclusions

This report presents the characterized neutron radiation environments for the free-field environment in the BP 1/5 of the NETL TRIGA reactor. The characterized location is 128-inch into beam port 1/5 loaded from the entrance of beam port 1 or beam port 5. The designation for this location is NETL-FF-BP1/5-128-cca. A 640-energy group and 89-energy group neutron spectrum were calculated using a high-fidelity MCNP model of NETL. The neutron spectrum was adjusted to align more closely with neutron activation dosimetry. The adjustment was performed using the least-squares code LSL-M3, an SNL unreleased modified version of LSL-M2[9][12][14]. Neutron and total dose conversion factors are presented to facilitate the conversion of various dosimetry readings into radiation metrics desired by experimenters.

This article has been authored by an employee of National Technology & Engineering Solutions of Sandia, LLC under Contract No. DE-NA0003525 with the U.S. Department of Energy (DOE). The employee owns all right, title and interest in and to the article and is solely responsible for its contents. The United States Government retains and the publisher, by accepting the article for publication, acknowledges that the United States Government retains a non-exclusive, paid-up, irrevocable, worldwide license to publish or reproduce the published form of this article or allow others to do so, for United States Government purposes. The DOE will provide public access to these results of federally sponsored research in accordance with the DOE Public Access Plan.

## References

- [1] D.R. Redhouse (2023), W.S. Charlton, “Radiation Characterization Summary: NETL Beam Port 1/5 Free-Field Environment at the 128-inch Core Centerline Adjacent Location (NETL-FF-BP1/5-128-cca),” SAND2022-15938, Sandia National Laboratories, Albuquerque, NM, November 2022
- [2] ASTM E720-16 – “Standard Guide for Selection and Use of Neutron Sensors for Determining Neutron Spectra Employed in Radiation-Hardness Testing of Electronics,” ASTM Standard, Published 2016
- [3] IRDFF-II (2014), v1.03, March 3,2014, <https://www-nds.iaea.org/IRDFF/>
- [4] MCNP – “A General Monte Carlo N-Particle Transport Code, Version 6.1,” LA-UR-03-1987, Los Alamos, NM, April 2003
- [5] R. Capote, (2012), K. I. Zolotarev, V. G. Pronyaev, A. Trkov, “Updating and Extending the IRDF-2002 Dosimetry Library,” JAI 9, April 2012
- [6] K. R. DePriest (2004) and P. J. Griffin, “NuGET User’s Guide: Revision 0,” SAND2004-1567, Sandia National Laboratories, Albuquerque, NM, April 2004
- [7] K. R. DePriest (2006), P. J. Cooper, E. J. Parma, “MCNP/MCNPX Model of the Annular Core Research Reactor,” SAND Report SAND2006-3067, Sandia National Laboratories, Albuquerque, NM, May 2006
- [8] P. C. Fisher (1964), L. B. Engle, “Delayed Gammas from Fast-Neutron Fission of Th232, U233, U235, U238, and Pu239,” Physical Review, Vol. 134, Number 4B, pp. B796 – B816, 25 May 1964
- [9] P. J. Griffin (1994a), J. G. Kelly, and J.W. VanDenburg, “User’s Manual for SNL-SAND-II Code,” SAND93-3957, April 1994
- [10] P. J. Griffin (1994b), J. G. Kelly, and D. W. Vehar, “Updated Neutron Spectrum Characterization of SNL Baseline Reactor Environments,” SAND93-2554, April 1994
- [11] P. J. Griffin (2011a), C. D. Peters, and D. W. Vehar, “Recommended Neutron Dosimetry Cross Sections for the Characterization of Neutron Fields,” RADECS 2011 Proceedings, 2011
- [12] W.N. McElroy (1967), S. Berg, T. Crockett, R. G. Hawkins, “A Computer-Automated Iterative Method for Neutron Flux Spectra Determination by Foil Activation, Vol. II: SAND-II (Spectrum Analysis by Neutron Detectors II) and Associated Codes,” AFWL-TR-67-41, September 1967
- [13] E. J. Parma (2014), T. J. Quirk, L. L. Lippert, P. J. Griffin, G. E. Naranjo, and S. M. Luker, “Radiation Characterization Summary: ACRR 44-Inch Lead-Boron Bucket Located in the Central Cavity onf the 32-Inch Pedestal at the Core Centerline (ACRR-LB44-CC-32-cl),” SAND13-3406, April 2013
- [14] F. W. Stallmann (1985), “LSL-M2: A Computer Program for Least-Squares Logarithmic Adjustment of Neutron Spectra,” NUREG/CR-4349, ORNL/TM-9933, March 1985
- [15] A. Trkov, P.J. Griffin, S.P. Simakov, et. al, “IRDFF-II: A New Neutron Metrology Library,” Nuclear Data Sheets, Vol. 163, pg. 1-108, January 2020
- [16] General Atomics (2021), “TRIGA History,” January 2020, <https://www.ga.com/triga/history>